



Study of the adsorptive properties of poly(1-methylpyrrol-2-ylsuaraine) particles in relation to small organic molecules – phenol, maleic acid, pyridine and paraquat

Daniel E. Lynch^{1*}, Martyna A. Radda², Mark J. Bateman²

¹Exilica Limited, The Technocentre, Puma Way, Coventry CV1 2TT, UK.

²Faculty of Engineering, Environment and Computing, Coventry University, Priory Street, Coventry CV1 5FB, UK.

³Semlalia Faculty of Science, Cadi Ayyad University, Av. My Abdellah, BP 2390, Marrakech, Morocco

Received 11 Aug 2019,
Revised 21 Jan 2020,
Accepted 25 Jan 2020

Keywords

- ✓ Polysuaraine,
- ✓ Adsorption,
- ✓ Particle,
- ✓ Phenol,
- ✓ Paraquat.

d.lynch@exilica.co.uk;
Phone: +447792004682

Abstract

The adsorption of aqueous solutions, at four different concentrations, of phenol, maleic acid, pyridine and paraquat into poly(1-methylpyrrol-2-ylsuaraine) (or PMPS) particles has been studied in both batch and column experiments and compared against concurrent experiments with granular activated carbon. All data for the batch experiments were fitted against linear, Langmuir and Freundlich adsorption models, although not all PMPS data was compliant. In terms of overall adsorption capacity for the first three organic analytes, the results presented in this study suggested that PMPS particles were not as capable as granular activated carbon, although the results for pyridine were comparable. However, PMPS particles were significantly better in their adsorption capacity of paraquat over the specific type of granular activated carbon used. The results obtained for the four organic analytes allowed for the rudimentary development of a model encompassing the adsorption characteristics of PMPS particles with respect to small molecule organic molecules.

1. Introduction

Adsorption is a process, which plays a significant role in industry in removing contaminants from a product as well as a direct means of recovery of valuable substances. It is extensively used for organic impurities removal from polluted sources, and it is widely applied in the mining industry in metallurgical operations for the concentration of valuable metals. Adsorption processes have found application in drinking water treatment for taste, odour and colour control, which are mainly effected by synthetic organic chemicals [1]. Some of which in waste waters and runoff can have carcinogenic effects (such as pesticides, herbicides, and organic solvents). Thus, the removal of these pollutants can be of particular significance to the environment and can also be an important objective in some industries.

The majority of water treatment applications involve physical adsorption [2] and there are basically three kinds of commercially available adsorbents used in adsorption processes for drinking water treatment: zeolites (aluminosilicates with varying ratio of Al to Si), synthetic polymeric adsorbents, and activated carbon. The most common of these used in water reclamation is activated carbon [2] being a versatile adsorbent material that is most effective in removing a wide spectrum of organic contaminants from water. However, this should not preclude research into investigating new generational adsorbent materials that offer alternative properties to activated carbon. Generally adsorbent materials are utilised in water treatment in either batch or continuous flow processes [3] so any new materials under investigation need to be able to be applied in these two processes.

Poly(1-methylpyrrol-2-ylsquaraine) (or PMPS) (Figure 1) particles can be precipitated from reaction solution (the polycondensation of equimolar amounts of 1-methylpyrrole and squaric acid in butanol) as 1.3 - 4 μm diameter blue-black spheres [4,5]. Of the studies on these particles during the 50 years from their initial reported synthesis in 1965 to 2015 [4-13], only three presented results that eluded to their potentially porous nature [5,12,13]. This was proven in 2015 with publication of an extensive study reporting the adsorption details of fifty-one metal elements coupled with images of their elaborate internal porous network [14]. This paper was followed up by an equally extensive study utilizing each of the porosity, size and shape characteristics of the particles to create metal compound core – silica shell materials of sixty-one metal elements [15]. However, in contrast to the examination and application of metal element adsorption into PMPS particles there have also been two recent studies on the PMPS adsorption of water (humidity) [16] and organic molecules, such as the removal of estradiol-type (Figure 1) endocrine disruptors from aqueous solution [17], which showed results compatible to activated carbon.

In order to begin to gain a better understanding of the adsorptive properties that PMPS particles could potentially have toward a broader range of organic molecules the authors decided to study the adsorption of phenol, maleic acid, pyridine and methyl viologen (or paraquat) (Figure 1) in PMPS particles from aqueous solution. Three of these four small organic molecules have some significance to wastewater treatment thus their adsorptive properties in activated carbons and other adsorbents are well known (for example: [18-27]). For this reason, batch adsorption experiments were run concurrently with granular activated carbon to act as both a direct comparison of PMPS performance as well as to verify that the experimental methodology was effective because all data from the activated carbon was expected to fit the three adsorption models (linear, Langmuir and Freundlich) that were employed on the equivalent PMPS data. Furthermore, all four chosen organic analytes represent differing types of organic molecules and their adsorption data was expected to lay the foundations of an adsorptive model for PMPS particles that would guide further adsorption studies. Subsequently, the aim of this current work was not to just measure the adsorption capacity of PMPS particles for phenol, maleic acid, pyridine and paraquat in aqueous solution and compare against the equivalent capacities of activated carbon, although that has been done, the aim additionally encompasses the beginnings of construction of a model that can be applied to an understanding of organic molecule uptake into PMPS particles from aqueous media. Such a model may have significance with respect to the adsorption and/or separation of biologically or pharmaceutically active molecules from wastewaters and effluent streams.

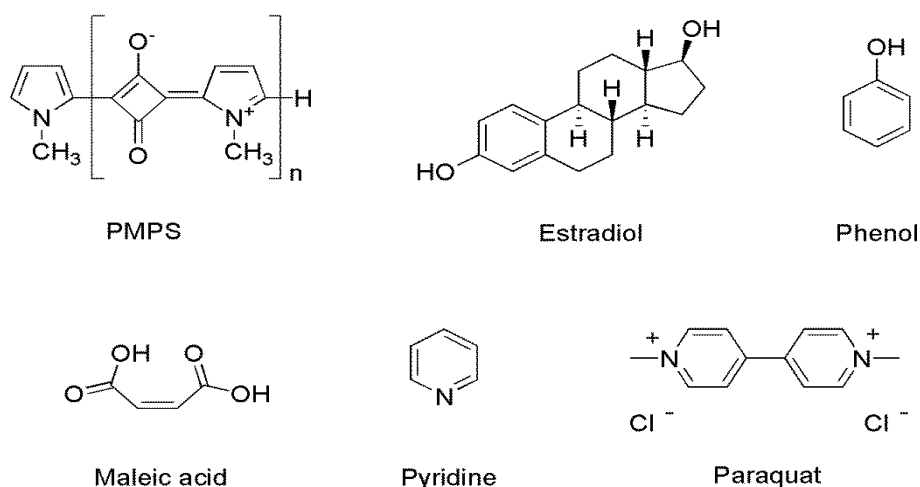


Figure 1: Molecular structures

2. Experimental

2.1. Chemicals and materials

All chemicals were purchased from Sigma-Aldrich and were used as-received. All water used in this study was reverse osmosis water. Poly(1-methylpyrrol-2-ylsquaraine) particles were prepared according to the literature procedure [10] by refluxing equimolar amounts of squaric acid and 1-methylpyrrole at a concentration of 175 mmol.L^{-1} in 2.5 L butanol for 6 h, filtering, and then washing (using a Soxhlet extractor) with hot ethyl acetate for 4 h before drying in a heated cabinet (60°C). The activated carbon used in this study to compare PMPS results against was Darco granular activated carbon with 20 - 40 mesh (1.27 - 0.635 mm) diameters.

2.2. Instrumentation

A Hewlett Packard Series 1050 high performance liquid chromatographic (HPLC) system was used for the quantitative measurement of all organic analytes. The specific analytical conditions for each organic analyte and determination of equipment and experimental accuracy are detailed in Supplementary material.

2.3. Batch and adsorption experiments

Six amounts ($0.0500\text{g} \pm 7\%$) of either PMPS particles or activated carbon were individually added to six cylindrical glass vials (with screw lids) followed by 10 mL aliquots of the standard solutions of 0, 25, 50, 100, 150, and 200 mg.L^{-1} for each organic analyte. All vials were sealed and then shaken for 18 h on a Stuart Orbital Shaker at the sixth speed level at room temperature (22°C). Upon completion, all solutions were gravity filtered through Whatman No. 42 filter papers before analysis on the HPLC. Treatment of data is detailed in Supplementary material.

2.4. Column adsorption experiments

Small scale columns were constructed using Pasteur pipettes, (145 mm length, D810, Volac Disposable Glass) produced by John Poulten Ltd, with the majority of the narrow spout removed to eliminate resistance to flow. Columns were constructed by first fitting a small rolled up ball of glass wool into the narrowing part of the pipette shoulder followed by packing accurately weighed PMPS particles (~ 150 mg), suspended in water, into the pipette to an approximate height of 4 cm. Each column was left overnight (16 h) to allow the material to gravity settle. All columns were attached to an 880PU Intelligent HPLC pump and tested with water to maintain a flow rate of 0.5 mL.min^{-1} . Satisfactory columns were then subjected to flow from the 200 ppm stock solutions, except for paraquat (100 ppm solution), with subsequent eluent analysis being taken at every 5 or 10 minutes (dependent upon exhaustion rate of the column) and analysed immediately by HPLC. Treatment of data is detailed in Supplementary material.

2.5. Equilibrium experiments

For phenol, maleic acid and pyridine, $0.0500 \text{ g} \pm 1.5\%$ portions of PMPS particles were placed in 12 glass vials (with sealable lids). 10 mL of the 200 mg.L^{-1} solution was added to each vial with initiation of a stopwatch. The vials were sealed, agitated (Stuart orbital shaker) for a set time and the mixture filtered through filter paper, with the analyte concentration in the subsequent filtrate being measured by HPLC. Time periods ranging from 30 s to 24 h were employed. Shorter time period experiments below 30 mins were run sequentially whereas longer time period experiments could be run concurrently. For paraquat, $0.0250 \text{ g} \pm 7\%$ portions of PMPS particles were used with 10 mL of the 100 mg.L^{-1} solution.

3. Results and discussion

3.1 Batch studies – equilibrium sorption capacity

The data collected throughout the batch adsorption studies for all four organic analytes enabled the presentation of analyte removal effect of the two examined adsorbents and their sorption capacities. These results for each analyte are shown graphically in Figure 2 and Figure 3 respectively. This data was subsequently used for the preparation of linear isotherms following Henry's law, and both Langmuir and Freundlich isotherms (as described in Supplementary material) for the four different organic analytes. The constants determined from each isotherm are given in Tables 1 – 3.

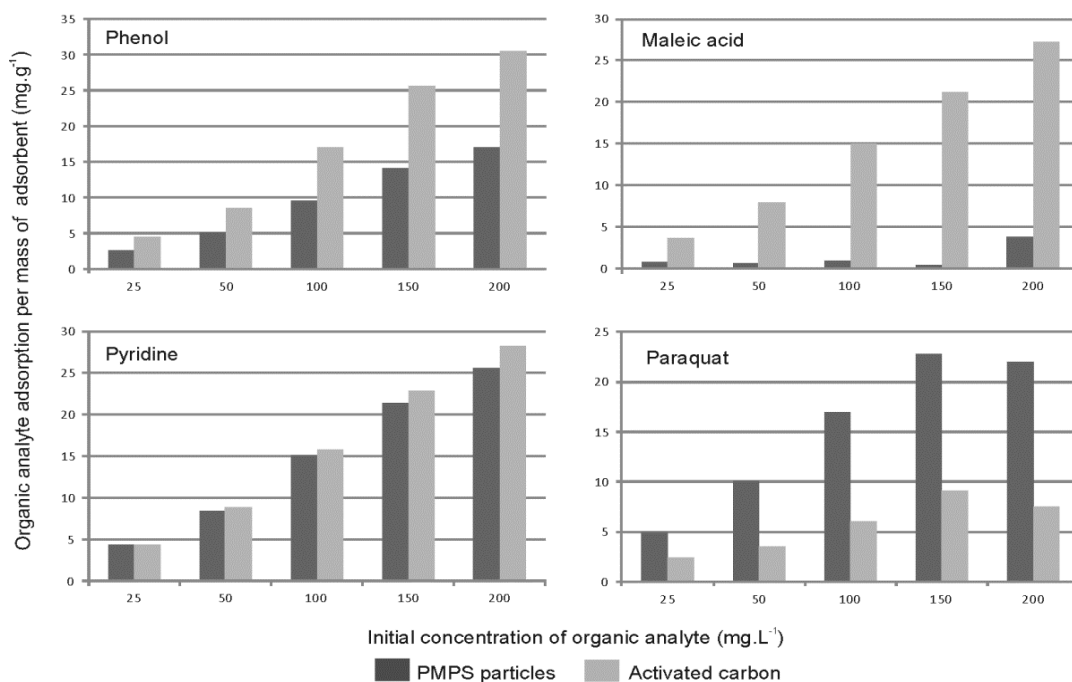


Figure 2: Weight of organic analyte adsorbed per mass of adsorbent for each of the five concentrations of organic analyte.

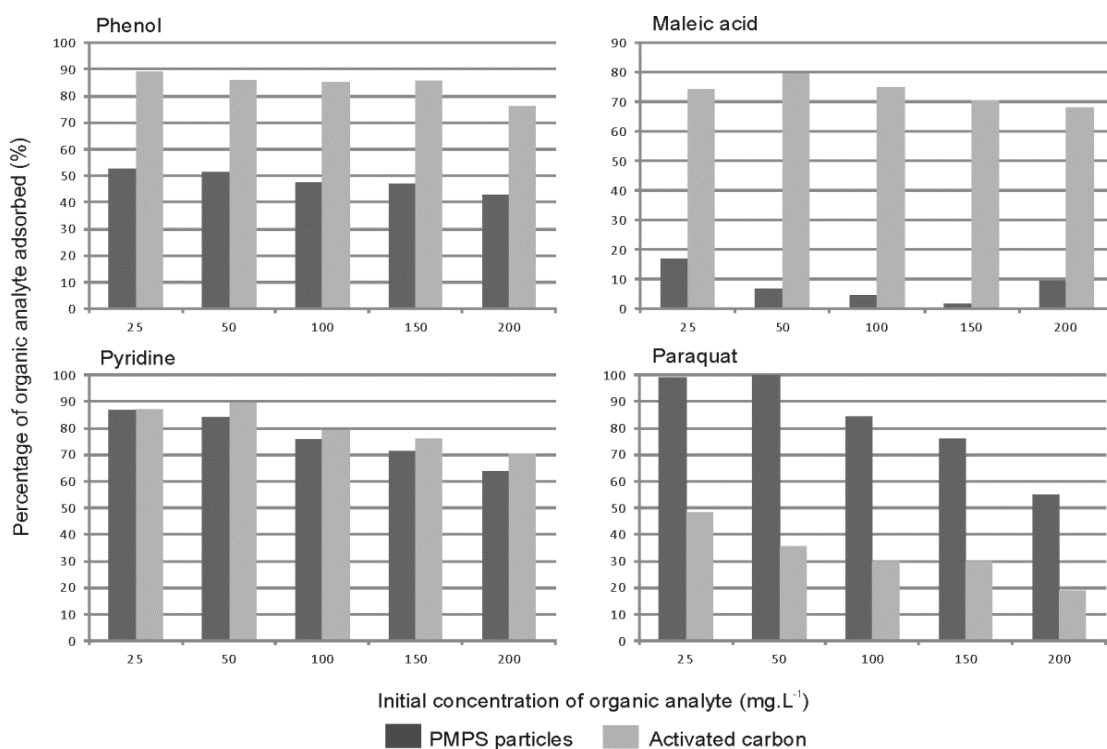


Figure 3: Percentage of organic analyte adsorbed for each of the five concentrations of organic analyte.

Figure 2 shows the raw adsorption data for weight of organic analyte adsorbed per mass of adsorbent for each of the five initial concentrations of organic analyte for each of the four organic analytes; phenol, maleic acid, pyridine and paraquat. In general, adsorption amount (per unit mass of adsorbent) increases with increased solution concentration, except for paraquat, which peaks at the penultimate concentration. A more relevant representation of sorption efficiency is shown in Figure 3, which shows the percentage of organic analyte adsorbed for each of the five initial concentrations of organic analyte for each of the four organic analytes. This figure shows that the adsorption efficiency of the specific type of activated carbon used in this study, for the adsorption of phenol, maleic acid and pyridine, ranges between just below 70% to almost 90% adsorption, whereas for paraquat, is much less efficient with adsorption ranging from just below 20% to just below 50%, for all organic analyte concentrations. This latter result for paraquat appears to be specific to this type of activated carbon because previous reported activated carbon adsorption capacities for this molecule are significantly higher (90 mg/g) [28].

Adsorption results for PMPS particles favour the two basic molecules (pyridine and paraquat), with all adsorption levels above 50% of available analyte, as opposed to levels of just over 50% or below for the two acid molecules (phenol and maleic acid) with a distinct difference between adsorption performance of the two. This preference for the uptake of adsorbents with inherent basicity in PMPS particles contrasts with recent results that show good uptake (> 85%) of endocrine disruptors of the estradiol class [17], which are slightly acidic (with pKa values that are analogous to phenol, being ≥ 10), and at pH = 4 adsorb these molecules with ~95% efficiency. This would indicate that molecule acidity / basicity is not the only factor in the prediction of PMPS adsorption efficiency. The high adsorption in PMPS particles of particular types of small molecules is comparable to a previous study on metal ion adsorption in these particles with adsorption preference given to the Lewis borderline and soft metal ions [14].

3.2 Linear adsorption isotherm model

The distribution of each analyte between the solid and liquids phases can be expressed by the distribution coefficient (or equilibrium coefficient) K_d , determined by the linear adsorption isotherm model, following Henry's Law (as detailed in Supplementary material). K_d is determined from the slope of the isotherm (going through zero) from plotting the loading of the analyte on the adsorbent [$\text{mg}\cdot\text{mg}^{-1}$] versus the analyte concentration in water in equilibrium [$\text{mg}\cdot\text{dm}^{-3}$], as shown in Figure 4. All isotherms, except the data for paraquat in PMPS particles, could be loosely fitted to this model. K_d values for each of the fitted isotherms are listed in Table 1. High values of K_d show the highest tendency of analyte passing from the liquid phase into the solid phase through sorption processes, whereas low K_d values indicate that there are larger amount of analyte remaining in the solution. For phenol, maleic acid and pyridine the highest K_d values were obtained for activated carbon, confirming that it has better adsorption capabilities for these three analytes. The simplicity of the linear model means that adsorbents with a steeper isotherm are, in general, more efficient in column applications than those with a flatter isotherm. It also means that adsorptive capacity increases at higher equilibrium analyte concentrations than at lower.

3.3 Langmuir adsorption isotherm model

Fitting the data to the Langmuir adsorption isotherm model required the plotting of the overall inverse of the mass of analyte adsorbed (x) [mg] divided by the adsorbent mass (m) [mg], i.e. $(x/m)^{-1}$ versus the inverse of the analyte concentration remaining in solution upon completed adsorption (C) [$\text{mg}\cdot\text{dm}^{-3}$], i.e. C^{-1} , as detailed in the Supplementary material. Two constants were thus determined from a rearranged form of the Langmuir equation, a and b , where the slope of each isotherm, shown in Figure 5, is $(ab)^{-1}$ and the intercept is b^{-1} . Two sets of data, both maleic acid and paraquat uptake in PMPS particles, could

not be fitted using this model. Furthermore, only three points for paraquat could be calculated due to the two lower concentration solutions undergoing near 100% adsorption.

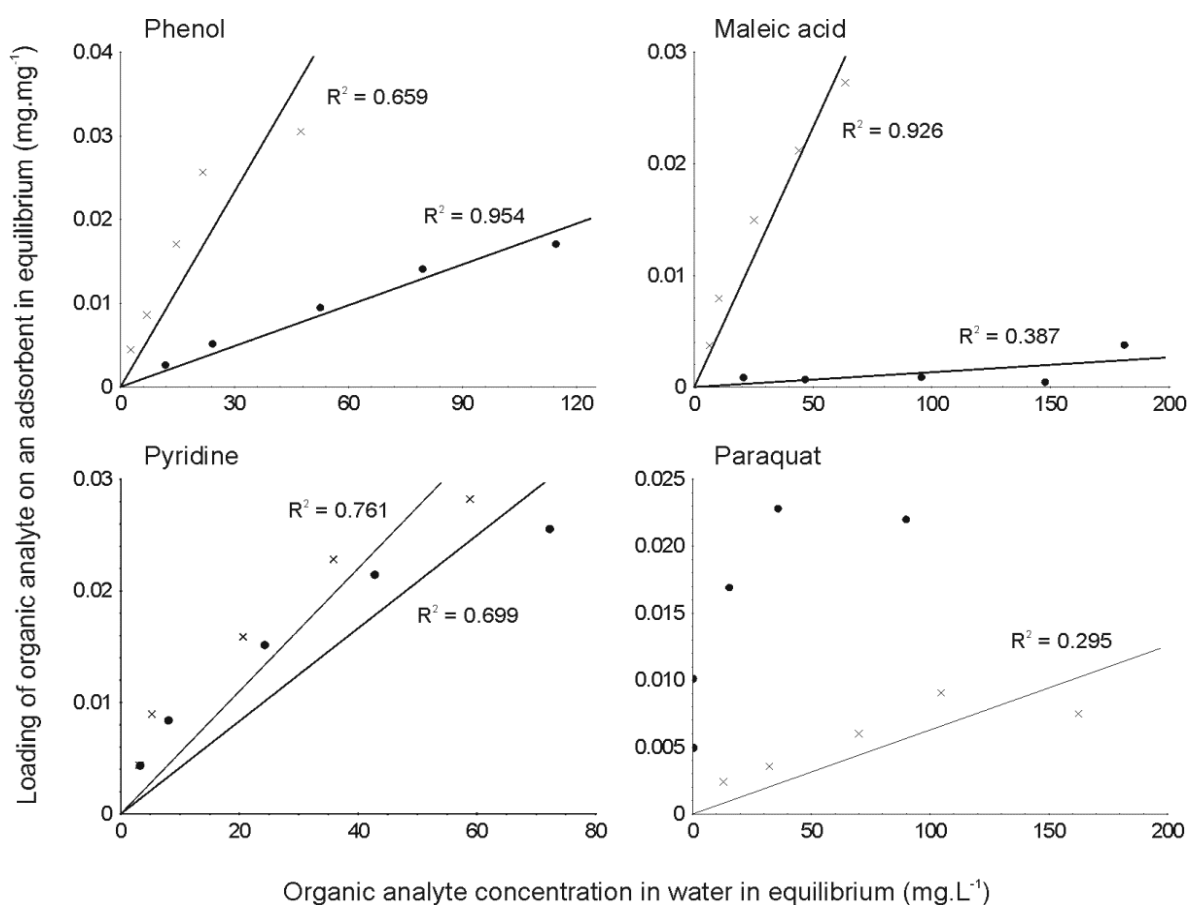


Figure 4: Loading of the analyte on the adsorbent versus the analyte concentration in water in equilibrium (● PMPS; × activated carbon).

Table 1: Distribution coefficients for each of the fitted linear isotherms from Figure 4.

Adsorbent	Analyte	Distribution coefficient K_d [dm ³ .mg ⁻¹]
PMPS particles	Phenol	1.63×10^{-4}
	Maleic acid	1.33×10^{-5}
	Pyridine	4.16×10^{-4}
Activated carbon	Phenol	8.78×10^{-3}
	Maleic acid	4.66×10^{-4}
	Pyridine	5.50×10^{-4}
	Paraquat	6.28×10^{-5}

Table 2 lists the equation of a straight line plus constants a and b for each of the fitted Langmuir isotherms in Figure 5. All fitted isotherms shown in this figure have $R^2 > 0.9$. If only three points are used for a fitted isotherm for the adsorption of paraquat in PMPS particles then the Langmuir equation becomes $(x/m)^{-1} = 281C^{-1} + 39.7$ with $R^2 = 0.846$, thus $a = 1.41 \times 10^{-1} \text{ dm}^3.\text{mg}^{-1}$ and $b = 2.52 \times 10^{-2} \text{ mg.mg}^{-1}$. Previously published results on the uptake of both phenol and pyridine in granular activated carbon with data treated using the Langmuir equation can be found in Wang *et al.* [18] and Lataye *et al.* [20] respectively, although units for x/m (referred to as q_e in both papers) are expressed as mg.g^{-1} and the equivalent of C is expressed in the former as mol.dm^{-3} .

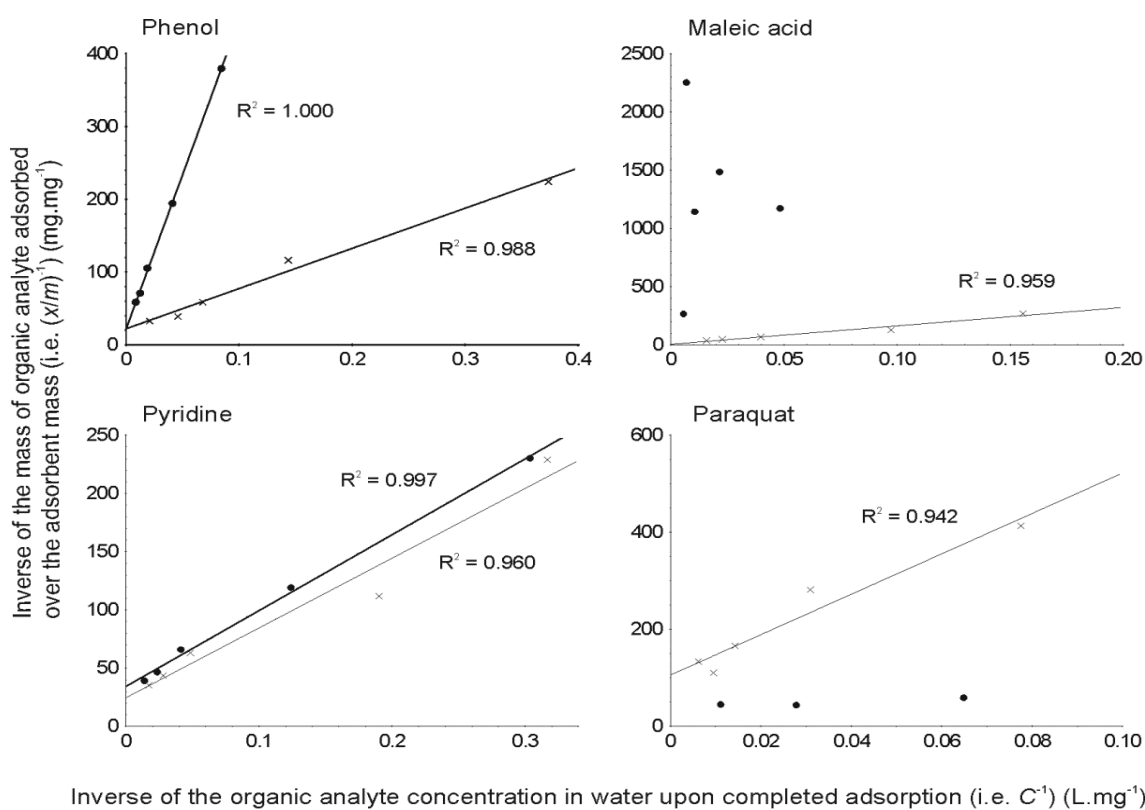


Figure 5: Langmuir isotherms (● PMPS; × activated carbon).

Table 2: Langmuir isotherm equations and constants for examined adsorbents

Adsorbent	Analyte	Langmuir equation	Constants	
			a [$\text{dm}^3.\text{mg}^{-1}$]	b [$\text{mg}.\text{mg}^{-1}$]
PMPS particles	Phenol	$(x/m)^{-1} = 4244C^{-1} + 20.9$	4.92×10^{-3}	4.78×10^{-2}
	Pyridine	$(x/m)^{-1} = 651C^{-1} + 34.3$	5.27×10^{-2}	2.92×10^{-2}
Activated carbon	Phenol	$(x/m)^{-1} = 552C^{-1} + 22.1$	4.00×10^{-2}	4.52×10^{-2}
	Maleic acid	$(x/m)^{-1} = 1581C^{-1} + 4.45$	2.81×10^{-3}	2.25×10^{-1}
	Pyridine	$(x/m)^{-1} = 599C^{-1} + 24.6$	4.11×10^{-2}	4.07×10^{-2}
	Paraquat	$(x/m)^{-1} = 4164C^{-1} + 106$	2.55×10^{-2}	9.43×10^{-3}

3.4 Freundlich adsorption isotherm model

Fitting the data to the Freundlich adsorption isotherm model required the plotting of $\log(x/m)$ versus $\log C$, as detailed in the Supplementary material. Again, two constants K (sorption capacity constant) [$\text{dm}^3.\text{mg}^{-1}$] and the dimensionless n (sorption intensity constant) can be determined from a rearranged form of the Freundlich equation where the slope of each isotherm, shown in Figure 6, is n^{-1} and the intercept is $\log K$. As per the Langmuir isotherm model, two sets of data, both maleic acid and paraquat uptake in PMPS particles, could not be fitted using this model. Again, only three points for paraquat could be calculated due to the two lower concentration solutions undergoing near 100% adsorption. Table 3 lists the equation of a straight line plus constants K and n for each of the fitted Langmuir isotherms in Figure 6. All fitted isotherms shown in this figure also have $R^2 > 0.9$. As per the previous section, if only three points are used for a fitted isotherm for the adsorption of paraquat in PMPS particles then the Freundlich equation becomes $\log(x/m) = 0.147\log C - 1.92$ with $R^2 = 0.628$, thus $K = 1.20 \times 10^{-2} \text{ dm}^3.\text{mg}^{-1}$ and $n = 6.80$. Phenol and pyridine adsorption data in granular activated carbon in Wang *et al.* [18] and Lataye *et al.* [20] were also treated to Freundlich analysis and can be used for comparison (taking into account the differing units).

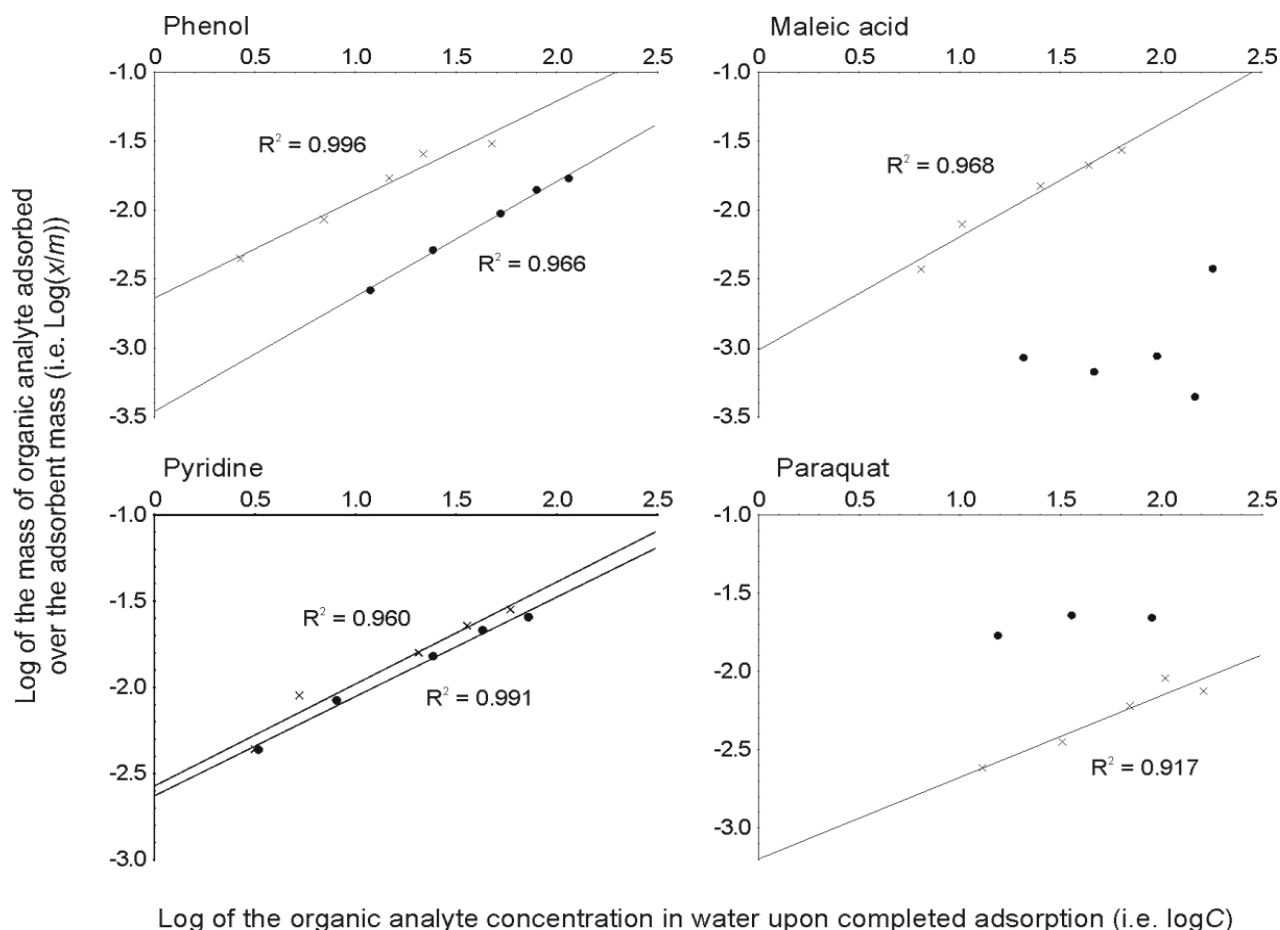


Figure 6: Freundlich isotherms (● PMPS; × activated carbon).

Table 3: Freundlich isotherm equations and constants for examined adsorbents

Adsorbent	Analyte	Freundlich equation	Constants	
			K [$\text{dm}^3 \cdot \text{mg}^{-1}$]	n
PMPS particles	Phenol	$\log(x/m) = 0.715\log C - 2.54$	2.88×10^{-3}	1.40
	Pyridine	$\log(x/m) = 0.577\log C - 2.63$	2.34×10^{-3}	1.73
Activated carbon	Phenol	$\log(x/m) = 0.834\log C - 3.46$	3.46×10^{-4}	1.20
	Maleic acid	$\log(x/m) = 0.821\log C - 3.01$	9.77×10^{-4}	1.22
	Pyridine	$\log(x/m) = 0.592\log C - 2.57$	2.69×10^{-3}	1.69
	Paraquat	$\log(x/m) = 0.521\log C - 3.20$	6.31×10^{-4}	1.92

3.5 Column studies – total sorption capacity

Determination of the total sorption capacity for each organic analyte in PMPS particles was undertaken by measuring the breakthrough volume of a solution of known concentration of each analyte that had been passed through a known weight of PMPS particles at a known flow rate. Column exhaustion was designated as being at the point at which the effluent concentration was 95% of the influent concentration (in three cases $190 \text{ mg} \cdot \text{L}^{-1}$ but $95 \text{ mg} \cdot \text{L}^{-1}$ for paraquat). Figure 7 shows the analyte concentration [$\text{mg} \cdot \text{L}^{-1}$] against time [mins] graphs for each analyte. From these graphs each of the total sorption capacities could be approximated, and are listed in Table 4. For phenol, maleic acid and pyridine adsorption into PMPS particles the 200 ppm solutions were within 10 – 15% of the 100 ppm solutions (Figure 3) but for paraquat, adsorption from the 200 ppm solutions was almost 30% lower than the 100 ppm solution, hence its use over the 200 ppm solution of this analyte in this part of the study.

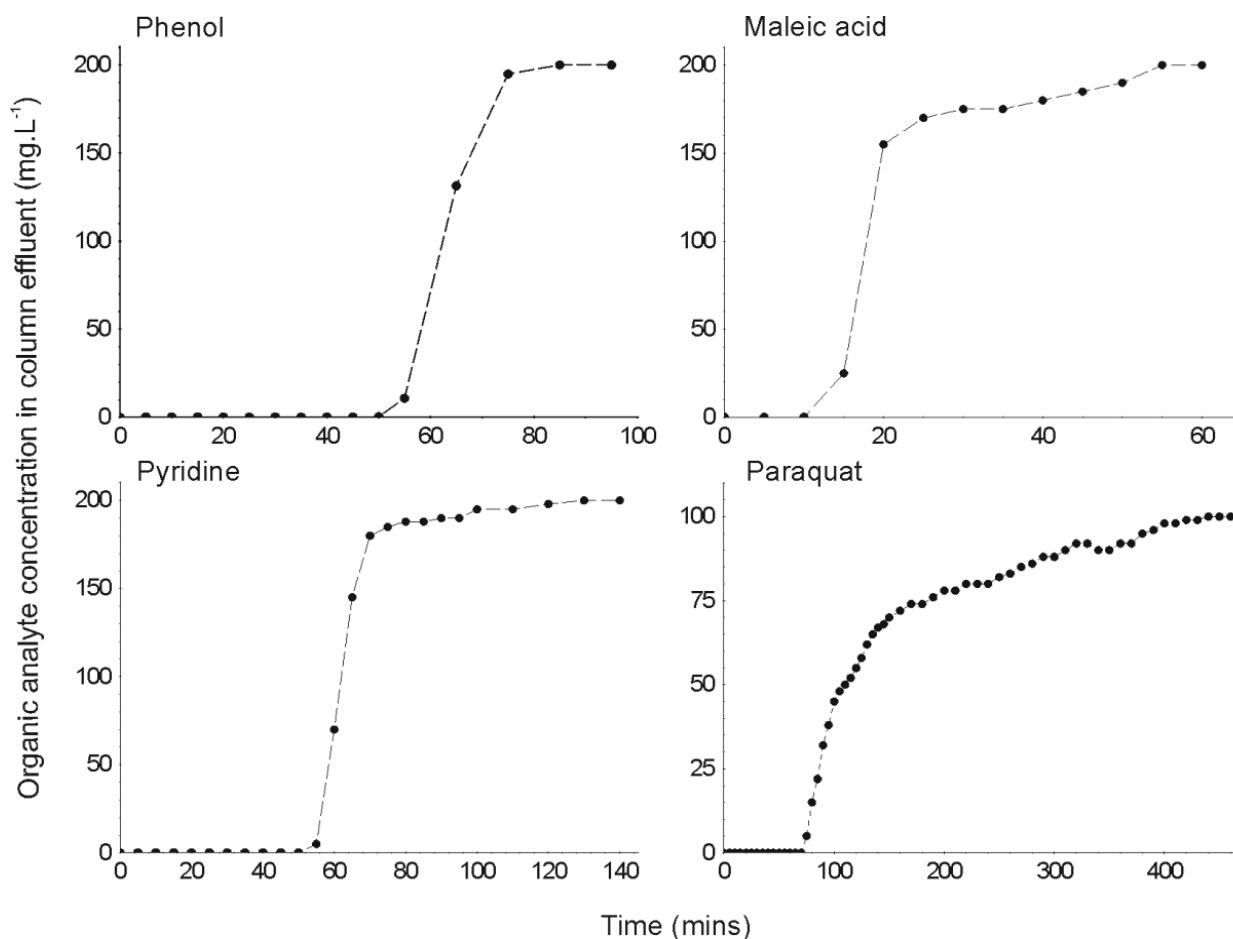


Figure 7: Column effluent organic analyte concentration versus time graphs for each analyte (PMPS only).

Table 4: Total approximated sorption capacity for each organic analyte in PMPS particles

Adsorbent	Analyte	Capacity [mg/g]
PMPS particles	Phenol	39.0
	Maleic acid	12.0
	Pyridine	39.2
	Paraquat	50.6

3.6 Equilibrium studies

Determination of the rate of adsorption of each organic analyte into the PMPS particles was undertaken by measuring the resultant concentration of each analyte solution following timed exposure to the PMPS particles. Figure 8 shows residual analyte concentration [mg.L^{-1}] against time [h] graphs for each analyte. These graphs give an indication of the time that each analyte takes to reach batch solution equilibrium. For both phenol and pyridine reaching equilibrium in batch solution would appear to be almost instantaneous with all available adsorption sites being filled as soon as the analyte comes into contact with the adsorbent. However, for maleic acid and paraquat that is not the case. For maleic acid the results would suggest that the adsorption process does not fall into a stable equilibrium. This is possibly because so little is adsorbed and numerous potential adsorption sites are available at any given time in the process. For paraquat, the majority of adsorption occurs instantaneously with continued adsorption occurring at a slower rate over several hours. This would indicate that the paraquat that is initially adsorbed slowly migrates deeper into the PMPS particle core thus making the outer sites available for more analyte. Some initial adsorption and release dynamics are also evident within the first hour of exposure to the analyte.

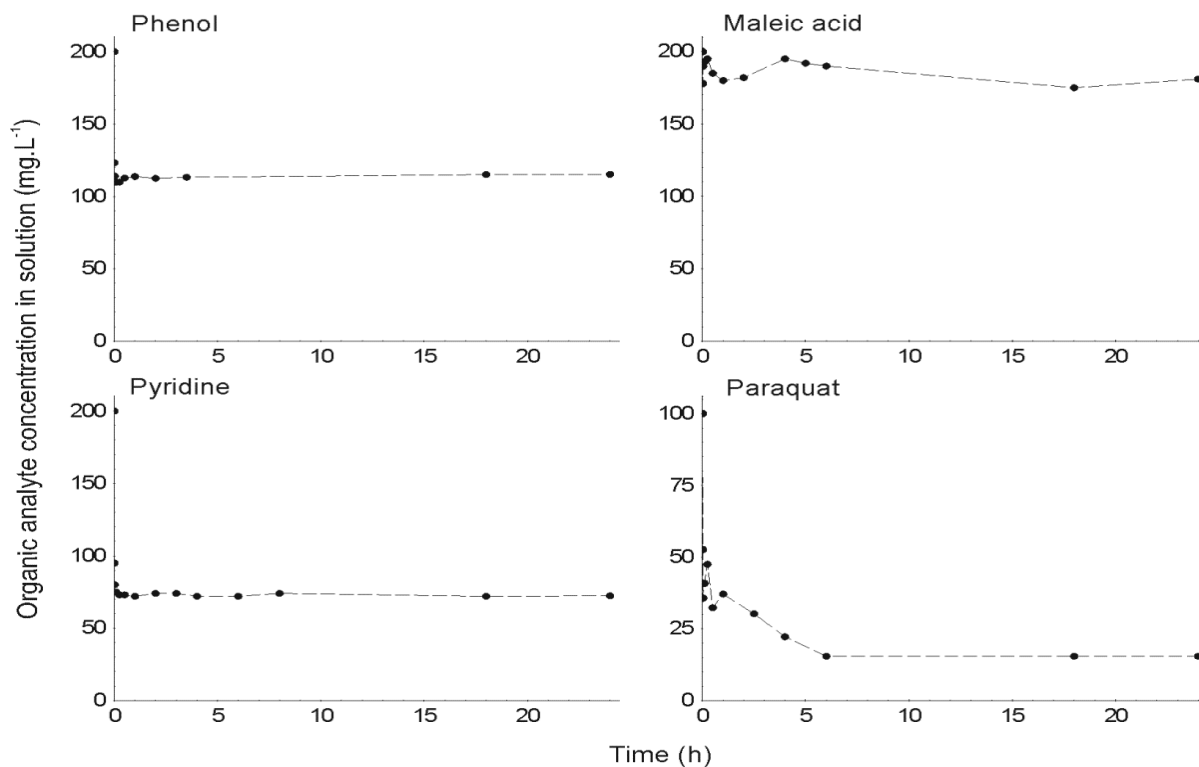


Figure 8: Residual organic analyte concentration versus time graphs for each analyte (PMPS only).

3.7 Discussion of PMPS particle adsorption properties

The aim of this paper, as mentioned in the Introduction, was not only to examine the adsorption capacity of PMPS particles for phenol, maleic acid, pyridine, and paraquat in aqueous solution but also that this particular choice of molecules could give additional information as to PMPS particle adsorption preferences with respect to small organic molecules. Both phenol and maleic acid are organic acids of differing acidic strength (i.e. differing pKa values). Pyridine and paraquat are both heterocyclic aromatic organic bases, although paraquat contains two quaternary nitrogen atoms. Phenol is an aryl alcohol whereas maleic acid is an aliphatic di-acid. Each of these compounds can interact with the PMPS molecular structure in different ways. The results presented in this paper would suggest that PMPS particles have a stronger sorption preference for organic bases over organic acids and aromatic compounds over aliphatic ones, although aliphatic bases have yet to be examined. This would certainly reinforce the results of the previous paper reporting estradiol adsorption [17], which contains both an aromatic ring plus several cyclic aliphatic rings. Maleic acid contains two carboxylic acid groups and is a much stronger acid than both phenol and estradiol but the lack of adsorption of maleic acid would suggest that hydrogen bonding associations with PMPS squarate oxygen atoms (Figure 9a) are not a strong contributor to PMPS sorption. In fact, the maleic acid graph in Figure 8 would suggest that hydrogen bonding associations alone in PMPS particle adsorption processes are weak and easily disrupted, as shown by the instability of maleic acid adsorption over time. Of stronger significance would appear to be aromatic to aromatic interactions such as $n - \pi$ and $\pi - \pi$ charge transfer associations (Figure 9b). The PMPS polymer backbone can be represented as a continuum of electron donor – acceptor regions (the pyrrolyl and squarate regions respectively) inductive to alignment with either type of ring system in an organic analyte. The adsorption behaviour of both phenol and pyridine into PMPS particles is similar with both essentially being weakly electron-donating aromatics and adsorbing to capacity almost instantaneously. Interesting adsorption behaviour is displayed by paraquat, which is not only a dual electron-accepting molecule but there is also the potential of electrostatic attraction between the positively charged quaternary paraquat nitrogen atoms and the negatively charged resonant squarate

oxygen atoms (Figure 9c). This interaction alone may be the reason why paraquat appears to penetrate deeper into the PMPS pores over time (as seen in the relevant graph in Figure 8).

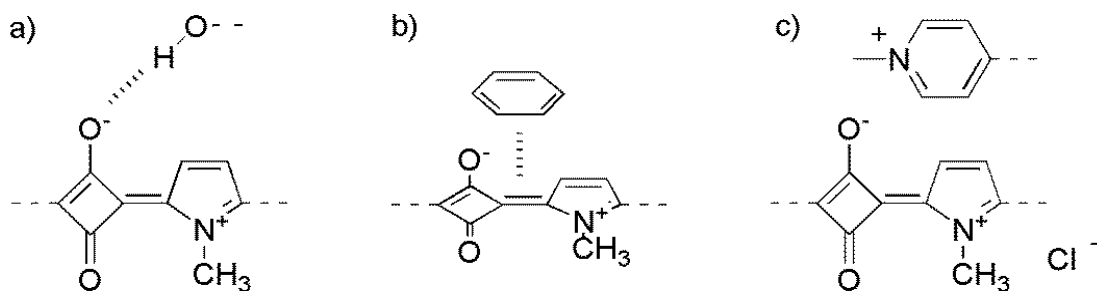


Figure 9: Three types of intermolecular associations that potentially contribute to PMPS adsorption of small organic molecules; a) hydrogen bonding, b) charge-transfer, and c) electrostatic.

Conclusion

In terms of overall adsorption capacity for phenol, maleic acid, and pyridine in PMPS particles in aqueous solution, the results presented in this study suggest that PMPS particles are not as capable as granular activated carbon, although the results for pyridine are comparable. However, PMPS particles are significantly better in their adsorption capacity of paraquat over the specific type of granular activated carbon studied herein. PMPS particles appear to favor the adsorption of basic organic molecules over acidic ones, although results are comparable if either type of molecule is capable of charge-transfer associations, i.e. contains some type of aromatic ring system, irrespective of whether that molecule (ring system) is electron-donating or electron accepting. Molecules containing multiple ring systems may also be favored for PMPS adsorption. In these cases the adsorption processes appear to fit known mathematical models. The strongest adsorption process in PMPS particles may be either an electrostatic association or a combination of charge-transfer and electrostatic.

Acknowledgements: The authors wish to thank the Faculty of Engineering, Environment and Computing and the Faculty of Health and Life Sciences, both of Coventry University, for financial assistance.

Supplementary material: This material is available free of charge via the Internet at <http://>

Conflicts of Interest: The authors declare no competing conflicts of interest. The use of PMPS particles as an adsorbent is covered by US patent 8,084,533.

References

1. N.P. Cheremisinoff, *Handbook of water and wastewater treatment technologies*, ISBN: 978-0-7506-7498-0 (2002).
2. J.C. Crittenden, R.R. Trussell, D.W. Hand, K.J. Howe, G. Tchobanoglous, *Water treatment: Principles and design*, ISBN: 978-0-470-40539-0 (2005).
3. W.J. Thomas, B. Crittenden, *Adsorption Technology & Design*, ISBN: 978-0-7506-1959-2 (1998).
4. D.E. Lynch, Y. Nawaz, T. Bostrom, The preparation of sub-micrometer silica shells using poly(1-methylpyrrol-2-yl)squaraine), *Langmuir*, 21 (2005) 6572-6575. <https://doi.org/10.1021/la0506933>
5. S. Begum, I.P. Jones, C. Jiao, D.E. Lynch, J.A. Preece, Characterisation of hollow Russian doll microspheres, *J. Mater. Sci.*, 45 (2010) 3697-3706. <https://doi.org/10.1007/s10853-010-4479-3>
6. A. Triebs, K. Jacob, Cyclotrimethine dyes derived from squaric acid, *Angew. Chem. Int. Ed.*, 4 (1965) 694. <https://doi.org/10.1002/anie.196506941>
7. A. Triebs, K. Jacob, Cyclobutenederivate der pyrrolreihe, *Liebigs. Ann. Chem.*, 699 (1966) 153-167. <https://doi.org/10.1002/jlac.19666990116>
8. L.P. Yu, M. Chen, L.R. Dalton, X.F. Cao, J.P. Jiang, R.W. Hellworth, Synthesis and characterization of third order nonlinear optical materials, *Mater. Res. Soc. Symp. Proc.*, 173 (1990) 607-612. <https://doi.org/10.1557/PROC-173-607>
9. U. Geissler, D.E. Lynch, N. Rohde, M.L. Hallensleben, D.J. Walton, Poly(oligo(1-methylpyrrole))s and their squaraine-derivatives: an electrochemical and spectrochemical investigation, *Synthetic Met.*, 84 (1997) 171-172. [https://doi.org/10.1016/S0379-6779\(97\)80698-4](https://doi.org/10.1016/S0379-6779(97)80698-4)
10. D.E. Lynch, U. Geissler, K.A. Byriel, An investigation into the electrical conduction properties of poly(oligo(1-methylpyrrol-2-yl)squaraine)s, *Synthetic Met.*, 124 (2001) 385-391. [https://doi.org/10.1016/S0379-6779\(01\)00376-9](https://doi.org/10.1016/S0379-6779(01)00376-9)

11. A.C. Sant'Ana, L.J.A. de Siqueira, P.S. Santos, M.L.A. Temperini, Vibrational characterization of poly(1-methylpyrrole-co-squaric acid) and poly(1-dodecylpyrrole-co-squaric acid) by enhanced Raman spectroscopy, *J. Raman Spec.*, 37 (2006) 1346-1353. <https://doi.org/10.1002/jrs.1544>
12. G.E. Spicer, D.E. Lynch, A.P. Newman, S.J. Coupe, The development of geotextiles incorporating slow-release phosphate beads for the maintenance of oil degrading bacteria in permeable pavements, *Water Sci. Technol.*, 54 (2006) 273-280. <https://doi.org/10.2166/wst.2006.580>
13. C. Courgneau, D. Rusu, C. Henneuse, V. Ducruet, M.F. Lacrampe, P. Krawczak, Characterisation of low-odour emissive polylactide/cellulose fibre biocomposites for car interior, *Express Polym. Lett.*, 7 (2013) 787-804. <https://doi.org/10.3144/expresspolymlett.2013.76>
14. D.E. Lynch, J.B. Bennett, M.J. Bateman, C.R. Reeves, The uptake of metal elements into poly(1-methylpyrrol-2-ylsquaraine) particles and a study of their porosity, *Adsorpt. Sci. Technol.*, 34 (2016) 176-192. <https://doi.org/10.1177/0263617415623426>
15. D.E. Lynch, A.C. Fellows, R. Wilcock, S. Sethi, S.C. Armour, L. Conteh, The use of poly(1-methylpyrrol-2-ylsquaraine) particles as a sacrificial template for the preparation of core-shell materials, *Mater. Chem. Phys.*, (2019) 163-169. <https://doi.org/10.1016/j.matchemphys.2019.02.013>
16. X. Xiao, Q.J. Zhang, J.H. He, Q.F. Xu, H. Li, N.J. Li, D.Y. Chen, J.M. Lu, Polysquaraines: novel humidity sensor materials with ultra-high sensitivity and good reversibility, *Sensor Actuat. B – Chem.*, 255 (2018) 1147–1152. <http://dx.doi.org/10.1016/j.snb.2017.04.069>
17. A.O. Ifelebuegu, H.T. Salauh, Y. Zhang, D.E. Lynch, Adsorptive properties of poly(1-methylpyrrol-2-ylsquaraine) particles for the removal of endocrine-disrupting chemicals from aqueous solutions: batch and fixed-Bed column studies, *Processes*, 6 (2018) 155. <https://doi.org/10.3390/pr6090155>
18. R.C. Wang, C.C. Kuo, C.C. Shyu, Adsorption of phenols onto granular activated carbon in a liquid-solid fluidized bed, *J. Chem. Tech. Biotechnol.*, 68 (1997) 187-194. [https://doi.org/10.1002/\(SICI\)1097-4660\(199702\)68:2<187::AID-JCTB651>3.0.CO;2-1](https://doi.org/10.1002/(SICI)1097-4660(199702)68:2<187::AID-JCTB651>3.0.CO;2-1)
19. N.K. Hamadi, S. Swaminathan, X.D. Chen, Adsorption of paraquat dichloride from aqueous solution by activated carbon derived from used tires, *J. Hazard. Mater.*, B112 (2004) 133–141. <https://doi.org/10.1016/j.jhazmat.2004.04.011>
20. D.H. Lataye, I.M. Mishra, I.D. Mall, Pyridine sorption from aqueous solution by rice husk ash (RHA) and granular activated carbon (GAC): Parametric, kinetic, equilibrium and thermodynamic aspects, *J. Hazard. Mater.*, 154 (2008) 858–870. <https://doi.org/10.1016/j.jhazmat.2007.10.111>
21. S.T. Hsu, L.C. Chen, C.C. Lee, T.C. Pan, B.X. You, Q.F. Yan, Preparation of methacrylic acid-modified rice husk improved by an experimental design and application for paraquat adsorption, *J. Hazard. Mater.*, 171 (2009) 465–470. <https://doi.org/10.1016/j.jhazmat.2009.06.144>
22. M. Brigante, G. Zanini, M. Avena, Effect of humic acids on the adsorption of paraquat by goethite, *J. Hazard. Mater.*, 184 (2010) 241–247. <https://doi.org/10.1016/j.jhazmat.2010.08.028>
23. C.P. Nansu-Njiki, G.K. Dedzo, E. Ngameni, Study of the removal of paraquat from aqueous solution by biosorption onto Ayous (*Triplochiton schleroxylon*) sawdust, *J. Hazard. Mater.*, 179 (2010) 63–71. <https://doi.org/10.1016/j.jhazmat.2010.02.058>
24. R. Ocampo-Perez, R. Leyva-Ramos, P. Alonso-Davila, J. Rivera-Utrilla, M. Sanchez-Polo, Modeling adsorption rate of pyridine onto granular activated carbon, *Chem. Eng. J.*, 165 (2010) 133–141. <https://doi.org/10.1016/j.cej.2010.09.002>
25. A. El-Sheikh, A.P. Newman, A.J. Said, A.M. Alzawahreh, M.M. Abu-Helal, Improving the adsorption efficiency of phenolic compounds into olive wood biosorbents by pre-washing with organic solvents: Equilibrium, kinetic and thermodynamic aspects, *J. Environ. Manag.*, 118 (2013) 1-10. <https://doi.org/10.1016/j.jenvman.2013.01.009>
26. J.O. Vinhal, M.R. Lage, J. Walkimar, M. Carneiro, C.F. Lima, R.J. Cassella, Modeling, kinetic, and equilibrium characterization of paraquat adsorption onto polyurethane foam using the ion-pairing technique, *J. Environ. Manag.*, 156 (2015) 200-208. <http://dx.doi.org/10.1016/j.jenvman.2015.03.022>
27. T. Fernandes, S.F. Soares, T. Trindade, A.L. Daniel-da-Silva, Magnetic hybrid nanosorbents for the uptake of paraquat from water, *Nanomaterials*, 7 (2017) 68. <https://doi.org/10.3390/nano7030068>
28. T. Meredith, J.A. Vale, in C. Bismuth, A.H. Hall (eds), *Paraquat Poisoning, Mechanisms, Prevention, Treatment (Drug and Chemical Toxicology)*, ISBN: 978-0824793708 (1995) 297-314.

(2020) ; <http://www.jmaterenvirosci.com>